Frequency-dependent seabed scattering on Browns Bank

Yan Jia and Robert Courtney
Geological Survey of Canada Atlantic

INTRODUCTION

Most marine seismic systems do not measure a calibrated estimate of the backscatter response of the seabed. To better predict the physical properties of the seabed, recent efforts at the Geological Survey of Canada Atlantic have attempted to bring a more quantitative approach to seismic surveying. Frequency-dependent seabed scattering was studied in a frequency domain from 1 to 6 kHz over two small areas with different surface conditions in Browns Bank (south of Yarmouth, Nova Scotia) using a broad-band, impulsive source and a calibrated hydrophone.

THEORY

A Huntec Deep Tow boomer was used as a point source in this study.

• source

r_1

• hydrophone (I_0 and I_1)

r_2

seabed

I_0 and I_1 are the calibrated source intensity and the scattered wave intensity recorded by hydrophone. The backscattering strength (BBS) is:

$$BSS = \log_{10} \frac{I_1}{I_0} \frac{(r_1+2r_2)^2}{r_1^2} \quad .$$

The backscattering coefficient m_{bs} [1] which is related to the back-scattering strength is defined as:

$$BSS = \log_{10} m_{bs} \, ,$$

$$m_{bs} = m_f + m_\mu + m_v \, ,$$

where m_f describes the scattering contribution from fine scale components of the bottom roughness,

$$m_f = M(k, \sigma_\mu) F(\delta_f, \theta_i) \, ,$$

$$M(k, \sigma_\mu) = R_0^2 \exp(-4\sigma_\mu^2 k^2 \cos^2 \theta_i) \, ,$$

$$F(\delta_f, \theta_i) = \frac{1}{8\pi\delta_f^2 \cos^2 \theta_i} \exp\left(-\frac{\tan^2 \theta_i}{2\delta_f^2}\right),$$

$$R_0 = \left[\frac{m\cos\theta_i}{(n^2-\sin^2\theta_i)^{1/2}} - 1\right] / \left[\frac{m\cos\theta_i}{(n^2-\sin^2\theta_i)^{1/2}} + 1\right]$$

where $k=\omega/c_1$ is the acoustic wave number, c_1 is the acoustic wave velocity in the sea water, f is the frequency, θ_i is the incident angle for the $i-th$ trace, σ_μ is the rms height of the micro roughness, δ_f is the rms slope of the fine-scale facets, and R_0 is the pressure-reflection coefficient of the seabed, $m=\rho_2/\rho_1$ (ρ_1 and ρ_2 are the densities of the water and sediment) and $n=c_1/c_2$ (c_1 and c_2 are the acoustic velocities of the water and sediment). m_μ is the contribution from the micro scale roughness,

$$m_\mu = R_0^2 k^4 \cos^4 \theta_i W\left(\frac{k}{\pi}\sin\theta_i\right) / \pi^2 \, ,$$

$$W\left(\frac{k}{\pi}\sin\theta_i\right) = a^2 \left(\frac{k}{\pi}\sin\theta_i\right)^{-2b} \, ,$$

where a and b are constants. m_v is the contribution from the inhomogeneities within the volume of the sediments,

$$m_v = \frac{160\pi m^2 m_0}{knK_p c_2 \ln 10} \, \frac{\cos^4(\theta_i-\alpha_f)\left[1-\frac{\sin^2(\theta_i-\alpha_f)}{n^2}\right]^{1/2}}{\{m\cos(\theta_i-\alpha_f)+[n^2-\sin^2(\theta_i-\alpha_f)]^{1/2}\}^4}$$

$$\alpha_f = \tan^{-1}\delta_f \, ,$$

where m_0 is the volume scattering coefficient, K_p is the attenuation factor for the compressional waves.

The unknown parameters θ_i, δ_f, σ_μ, a, b and K_p were the model parameters of the inversion for the BSS data.

DATA

Two areas with different surface conditions in Browns Bank were studied. The first area (Site 2) is a broadly smooth and it is covered by very coarse sand and gravel, while the other site (Site 3) has high amplitude bedforms, covered with medium to fine sand. The scattered wave amplitudes at Site 2 can be easy detected for every trace, while some seabed reflections on Site 3 are very weak and difficult to detect. Fig. 1 shows both high and low amplitude examples of scattered waveforms from each site.

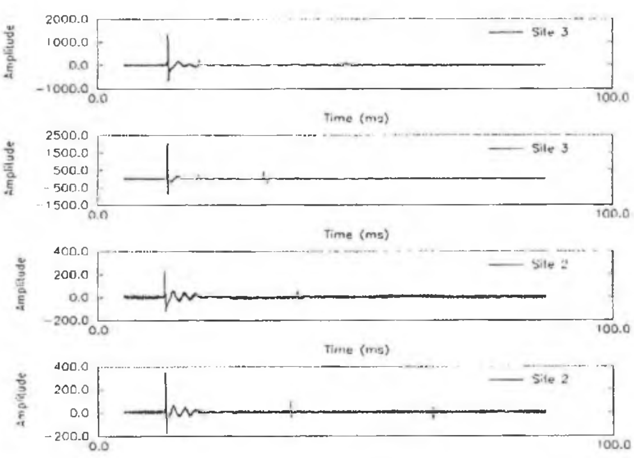

Fig. 1: The acoustic wave amplitudes of Site 2 and Site 3 recorded at the hydrophone

RESULTS AND DISCUSSION

Fig. 2 shows the measured BSS data as a function of frequency. The BSS data of Site 2 concentrate near -30 dB, while the data of Site 3 show a large variation at each frequency.

For the inversion, we used m=2.23, n=0.80 for Site 2 and m=1.45, n=0.90 for Site 3. As the velocity, we chose c_1=1480 m/s, c_2=1850 m/s for Site 2 and c_2=1639 m/s for Site 3. Table 2 lists the inversion results for two sites (file1, file2 for Site 2, and file21, file23 for Site 3). The volume scattering coefficients and the attenuation factors for these four files are similar. The last column in Table 2 describes the data variance of the inversion. In order to illustrate how well the inversion results fit the data, Fig. 3 gives four examples of the comparison between the real data and the theoretical data calculated from the inversion results. These four examples have derived incident angles around 10 degrees. At the same incident angle, the backscattering strength of the two files from Site 2 are significantly stronger than the other files from Site 3.

The inverted incident angles mostly vary between 5 and 20 degrees. There are some angles for Site 3 which are anomalously large. These estimates are likely less accurate due to the relatively higher noise contribution to the recorded signal at lower scattered amplitudes.

Table 2: Inversion results

	δ_f	σ_μ	a	b	mo	K_p*	σ^2_d
file1	1.47°	0.07	0.14	1.02	3.0e-6	0.100	0.02827
file2	1.28°	0.06	0.11	1.10	3.5e-6	0.096	0.02430
file21	1.00°	0.04	0.045	1.32	1.7e-5	0.099	0.01373
file23	1.03°	0.04	0.068	1.40	1.8e-5	0.099	0.03460

* units of dB/m/Hz.

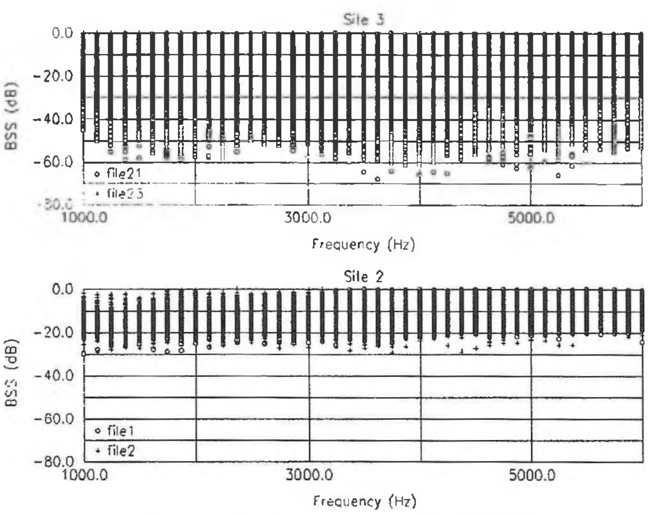

Fig. 2: The BSS results for Site 2 and Site3.

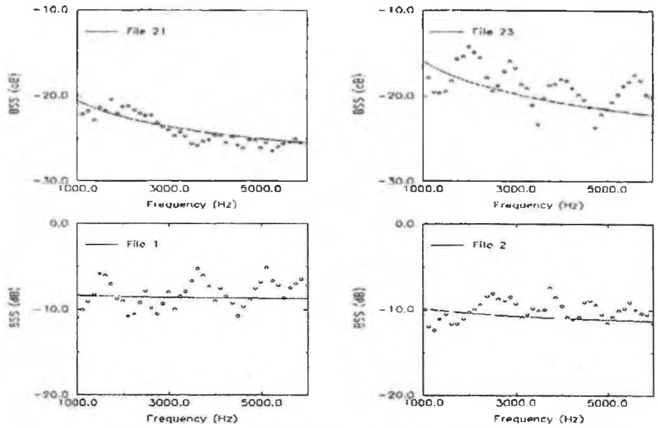

Fig. 3: Comparison between the theoretical values calculated from the inversion results and the measured data.

The apparent seabed bathymetry was calculated by integrating the incident angle information derived from the inversion. Fig. 4 shows examples of the comparison between the calculated seabed bathymetry and the seabed depths measured from the arrival times of the scattered waves. The calculated estimates are close those derived from measured arrival times.

CONCLUSION

The backscattering strength is largely dependent on the gradient of the long-wavelength bathymetry and the in-situ values of the primary geo-acoustic parameters (e.g, velocity and density). Near-normal incidence acoustic parameters (δ_f, σ_μ) and volume scattering coefficient (m_o) have less effect on the scattered signal and show little relative variation for the sites examined in this study.

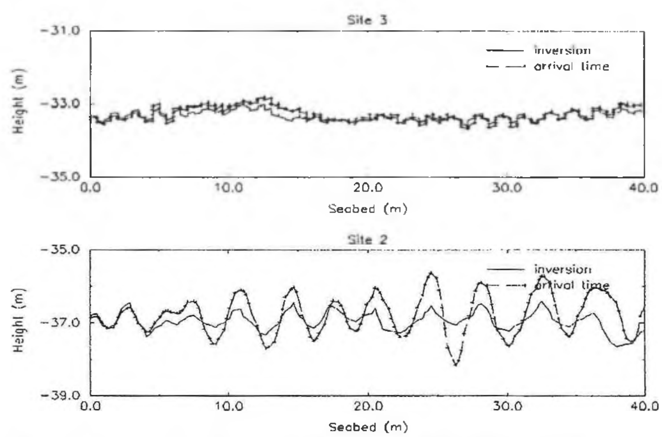

Fig. 4: The simulated seabed shape is similar to the seabed bathymetry estimated by the arrival time of the scattered waves.

REFERENCE

[1] J. C. Novarini and J. W. Caruthers, "A simplified approach to backscattering from a rough seafloor with sediment inhomogeneities," IEEE Vol. 23, pp 157-166 1998.